

See discussions, stats, and author profiles for this publication at: <https://www.researchgate.net/publication/243375027>

Synthesis and Hole-Transporting Properties of Highly Fluorescent N Aryl Dithieno[3,2- b :2',3'- d]pyrrole-Based Oligomers

ARTICLE *in* THE JOURNAL OF PHYSICAL CHEMISTRY C · MARCH 2010

Impact Factor: 4.77 · DOI: 10.1021/jp909064n

CITATIONS

11

READS

29

6 AUTHORS, INCLUDING:



Ganapathy Balaji

Iowa State University

20 PUBLICATIONS 254 CITATIONS

[SEE PROFILE](#)



Chellappan Vijila

Agency for Science, Technology and Rese...

69 PUBLICATIONS 627 CITATIONS

[SEE PROFILE](#)



Furong Zhu

Hong Kong Baptist University

155 PUBLICATIONS 2,560 CITATIONS

[SEE PROFILE](#)



Suresh Valiyaveettil

National University of Singapore

232 PUBLICATIONS 6,686 CITATIONS

[SEE PROFILE](#)

Synthesis and Hole-Transporting Properties of Highly Fluorescent N-Aryl Dithieno[3,2-*b*:2',3'-*d*]pyrrole-Based Oligomers

Ganapathy Balaji,[†] Manoj Parameswaran,[†] Tan Mein Jin,[‡] Chellappan Vijila,[‡] Zhu Furong,[‡] and Suresh Valiyaveettil*,[†]

Department of Chemistry, National University of Singapore, 3 Science Drive 3, Singapore 117543, Singapore, and Institute of Materials Research and Engineering, A-Star, 3 Research Link, Singapore 117602

Received: September 20, 2009; Revised Manuscript Received: January 19, 2010

A new series of dithieno[3,2-*b*:2',3'-*d*]pyrrole-incorporated oligomers was synthesized and characterized. The crystal structure, crystal packing, optical properties, electrochemical properties, and time-of-flight mobilities were investigated in detail. The oligomers are highly fluorescent in both solution and the solid state. The solution-state quantum yield of these new compounds ranged from 52 to 75%. Band gaps of these oligomers were found to be in the range of 2.5–2.8 eV. The surface morphology of the film was also characterized by atomic force microscopy. The material was found to be hole-transporting with a mobility on the order of $10^{-6} \text{ cm}^2/(\text{V s})$.

Introduction

Organic materials in electronic applications overcome many of the drawbacks of silicon technology such as expensive fabrication, difficulty in tuning the properties, and limited processability.¹ Generally, organic π -conjugated low molecular weight oligomers or highly defined polymers are used for such applications.² The advantage of oligomeric systems over the polymeric counterpart is their well-defined structures, high purity, and high processability. Oligomers are processable by either vacuum sublimation or solution casting.³ Among the π -conjugated materials, oligo- and polythiophenes are used in many of the optoelectronic applications such as organic light emitting diodes (OLEDs),⁴ organic field effect transistors (OFETs),⁵ and organic photovoltaics (OPVs).⁶

Fused thiophene systems like dithieno[3,2-*b*:2',3'-*d*]thiophene,⁷ cyclopenta[2,1-*b*:3,4-*b'*]dithiophene,⁸ and dithieno[3,2-*b*:2,3-*d*]-pyrrole^{9–17} are interesting due to their fused nature and enhanced π -conjugation¹⁰ and are used in various applications.¹¹ Dithieno[3,2-*b*:2,3-*d*]pyrrole (DTP) contains a pyrrole fused planar tricyclic system, similar to carbazole. It is known that such molecules offer better electron-donating properties than carbazole due to their lower ionization potential.¹² DTP-based copolymers with acceptor units lead to low band gap materials, which are realized in OPV¹³ and OFET¹⁴ applications.

Unfunctionalized and N-functionalized DTP molecules showed low quantum yields of ~ 0.008 and 0.1%, respectively.¹⁵ Therefore, DTP molecules with higher quantum yield and better transport property are crucial for extensive material applications. Rasmuseen and co-workers reported a high solution-state quantum yield, up to 65% for DTP-based oligomers and polymers.¹⁶ DTP-based copolymers also showed a high quantum yield in solution as well as in the solid state.¹⁷ To develop a better DTP-based fluorophore, *N*-aryl DTP is a more interesting building block than *N*-alkyl DTP, as the high-frequency mode

of relaxation which could promote the internal conversion in the alkyl analogue is absent in *N*-aryl DTP.

In this regard, we synthesized DTP-based oligomers with high quantum yield and studied their charge carrier mobility in detail. Four new oligomers were synthesized with the DTP core incorporated with fluorene, carbazole, triarylamine, and benzene groups. Their photophysical, electrochemical, surface morphology, and transport properties along with single-crystal X-ray studies (of DTP–TPA) are presented. Molecular structures of the synthesized molecules are shown in Figure 1.

Experimental Section

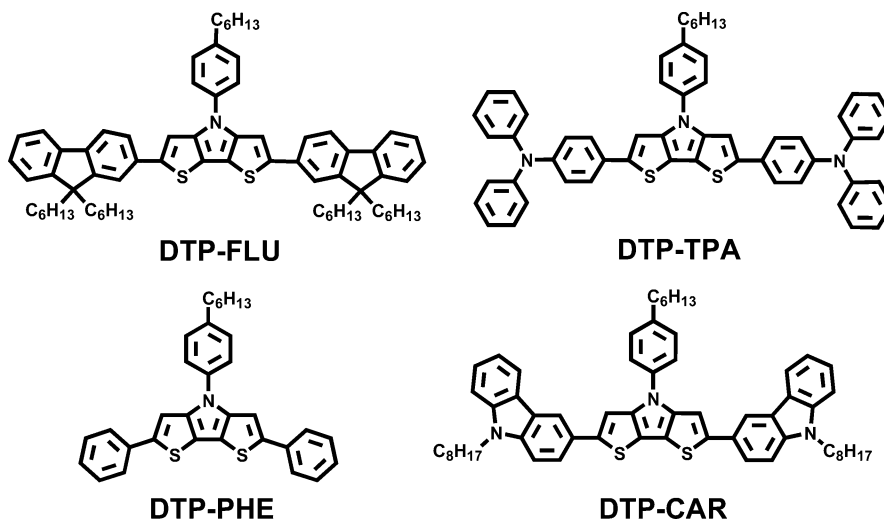
Materials. All reactions were carried out under an inert atmosphere (N_2 or Ar), unless specified otherwise. All reagents were used without further purification, unless otherwise stated. All reactions were carried out with freshly distilled anhydrous solvents under an inert atmosphere. Tetrahydrofuran (THF) was purified via distillation over sodium under a nitrogen atmosphere. NBS was recrystallized from hot water. *N*-(4-hexylphenyl)-2,6-dibromodithieno[3,2-*b*:2',3'-*d*]pyrrole was prepared following the literature procedure.¹⁸

Spectroscopic Characterization. ^1H (300 MHz) and ^{13}C (75 MHz) NMR spectra were recorded on a Bruker AMX 300 spectrometer. Mass spectra were acquired by a Micromass VG7035 double focusing mass spectrometer of high resolution. Single-crystal X-ray diffraction measurements were conducted on Bruker-AXS Smart Apex CCD single-crystal diffractometers. Unit dimensions were acquired with least-squares refinements, and all structures were solved by SHELXL-97. The UV-vis spectra were measured on a Shimadzu UV-1601 PC spectrophotometer, and fluorescence measurements were carried out on a RF-5301PC Shimadzu spectrofluorophotometer. Solution-state photoluminescence quantum yields were recorded using quinine sulfate (0.1 M H_2SO_4) as the standard.¹⁹ Spectroscopic-grade solvent (THF) was used for preparing sample solutions and checked for background fluorescence. The solution of each sample and standard at five different concentrations (each concentration was chosen to give an absorption of the sample less than 0.1 at the excitation wavelength) were analyzed. The absorbance and integrated fluorescence intensity values at each

* To whom correspondence should be addressed. Tel.: +65 - 6516 4327. Fax: +65 - 6779 1691. E-mail: chmsv@nus.edu.sg.

[†] National University of Singapore.

[‡] Institute of Materials Research and Engineering.

**Figure 1.** Structure of synthesized DTP oligomers.

concentration were obtained and plotted to get the gradient (*m*) with intercept = 0. The quantum yield value was calculated using the relation

$$\Phi_x = \Phi_s [\text{Gra X}/\text{Gra S}] [\eta_x^2/\eta_s^2]$$

where S and X denotes the standard and test sample, respectively. $\Phi_s = 54\%$ (quinine sulfate in 0.1 M H₂SO₄).

The solid-state quantum yield was determined using an integrating sphere (Lab Sphere Com) with a He–Cd laser (325 nm; 11 mW) as an excitation source. The surface morphology was studied using atomic force microscopy (AFM) working in the tapping mode. The experiment was performed at room temperature using a commercial AFM Nanoscope IV (Dimension 3100, Digital Instruments). The electrochemical behavior of the oligomers was investigated with cyclic voltammetry (CV). The cyclic voltammograms were recorded with a computer-controlled CHI Electrochemical Analyzer/Workstation CHI 600C at a constant scan rate of 100 mV/s. Measurements were performed in an electrolyte solution of 0.1 M tetrabutylammoniumhexafluorophosphate (*n*-Bu₄NPF₆) dissolved in degassed dichloromethane. An undivided three-electrode configuration cell was used with a Pt wire as the working and counterelectrode and Ag/AgCl as the reference electrode. The potentials were calibrated with a ferrocene/ferrocenium redox couple (0.47 V). The onset value of the oxidation wave ($E_{\text{ox}}^{\text{onset}}$) was used to calculate the energy level, using the relation $E_{\text{HOMO}} = -(4.38 + E_{\text{ox}}^{\text{onset}})$. LUMO levels were calculated from E_{HOMO} and optical band gaps (E_g).

The mobilities of the charge carriers were measured by using the time-of-flight photoconductivity technique. The system was composed of a pulsed nitrogen (N₂) laser (Oriel 79074), a pulse generator (SRS-DG535), a DC voltage source (Kenwood PWR18-2), and a digital oscilloscope (Agilent-Infinium, 1 GHz, 4 Gsa/s). The photocurrent under the influence of an applied electric field was monitored across a variable resistor using an oscilloscope. The mobilities of the charges were calculated using the relation $\mu = d^2/Vt_{\text{tr}}$, where *d* is the film thickness, *V* is the applied voltage, and *t_{tr}* is the transit time. The details of the setup have been described elsewhere.²⁰ All measurements were done in air at room temperature, and no detectable degradation was observed under repeated measurements.

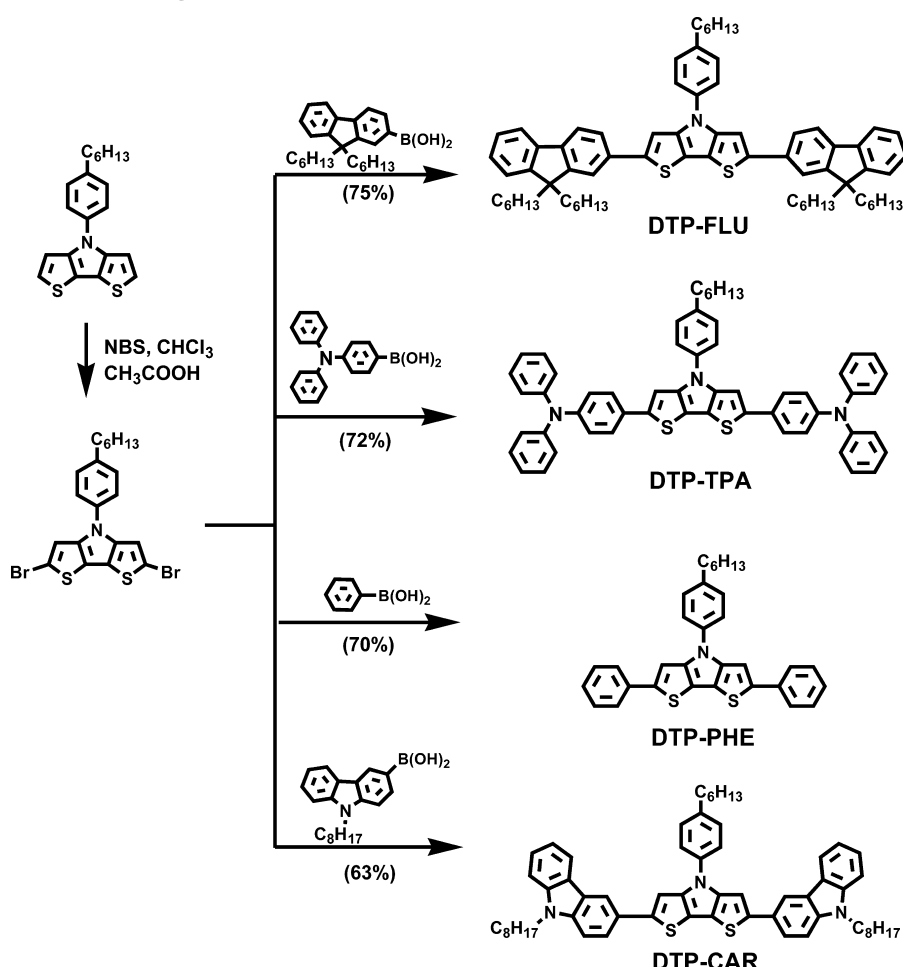
Synthesis of *N*-(4-Hexylphenyl)dithieno[3,2-*b*:2',3'-*d*]pyrrole.¹⁸ Toluene (40 mL), Pd₂(dba)₃ (887 mg, 1.54 mmol), P(Bu)₃HBF₄ (448 mg, 1.54 mmol), 3,3'-dibromo-2,2'-bithiophene (2.5 g, 7.72 mmol), NaO'Bu (2.23 g, 23.15 mmol), and 4-hexylaniline (1.92 g, 10.08 mmol) were used and yielded a pale-orange solid (1.7 g, 65%). ¹H NMR (300 MHz, CDCl₃, δ , ppm): 7.49 (d, *J* = 8.22 Hz, 2H, Ph–H), 7.32 (d, *J* = 8.22 Hz, 2H, Ph–H), 7.16 (s, 4H, Th–H), 2.68(t, *J* = 7.73 Hz, 2H, Ar–CH₂), 1.67 (m, 2H, CH₂), 1.35 (m, 6H, CH₂), 0.91(t, *J* = 6.57, CH₃). HRMS *m/z*: [M]⁺ calcd for C₂₀H₂₁NS₂, 339.1115; found, 339.1113.

Synthesis of 2,6-Dibromo-*N*-(4-hexylphenyl)dithieno[3,2-*b*:2',3'-*d*]pyrrole.¹⁸ Glacial acetic acid (20 mL), CHCl₃ (20 mL), DTP (1 g, 2.94 mmol), *N*-bromosuccinimide (1.31 g, 7.38 mmol) were used to produce a pale-yellow solid (1.13 g, yield 77%). ¹H NMR (300 MHz, CDCl₃, δ , ppm): 7.38 (d, *J* = 8.55 Hz, 2H, Ph–H), 7.31 (d, *J* = 8.52 Hz, 2H, Ph–H), 7.15 (s, 2H, Th–H), 2.67(t, *J* = 7.7 Hz, 2H, Ar–CH₂), 1.64 (m, 2H, CH₂), 1.35 (m, 6H, CH₂), 0.91(t, *J* = 6.57, CH₃). ¹³C NMR (75.4 MHz, CDCl₃, δ , ppm): 141.9, 140.9, 136.5, 129.9, 127.4, 122.8, 115.4, 110.3, 35.5, 31.7, 31.4, 29, 22.6, 14.1. HRMS *m/z*: [M]⁺ calcd for C₂₀H₁₉NBr₂S₂, 496.9305; found, 494.9324.

Representative Synthesis of DTP Oligomers. 2,6-Dibromo-*N*-(4-hexylphenyl)dithieno[3,2-*b*:2',3'-*d*]pyrrole (wt, 2 mmol) and the corresponding monoboronic acid (wt, 4.2 mmol) were dissolved in 40 mL of dry THF under N₂. To this solution, K₂CO₃(aq) (2 M, 30 mL; N₂ bubbled before use) and Pd(PPh₃)₄ (wt, 0.2 mmol) were added. After stirring for 6 h at 80 °C, the reaction mixture was cooled and extracted with water and ethyl acetate. The combined organic layer was dried with anhydrous sodium sulfate and concentrated under reduced pressure and purified by column using a 99:1 hexane/ethylacetate mixture as the eluent.

2,6-Bis[2-(9,9-dihexyl-9H-fluorene)]-*N*-(4-hexylphenyl)dithieno[3,2-*b*:2',3'-*d*]pyrrole (DTP-FLU). Yellow green solid (75%). Melting point: 65.6–67.4 °C. ¹H NMR (300 MHz, CDCl₃, δ , ppm): 7.71–7.5 (m, 10H, Ar–H); 7.44–7.3 (b, 10H, Ar–H); 2.75 (t, 7.71 Hz, 2H, Ar–CH₂), 2 (t, 7.4 Hz, 8H, Ar–CH₂), 1.73 (m, 2H, CH₂), 1.38 (m, 6H, CH₂), 1.06 (b, 32H, CH₂), 0.763 (b, 15H, CH₃). ¹³C NMR (75.4 MHz, CDCl₃, δ , ppm): 151.6, 150.9, 144.4, 144.3, 141.4, 140.7, 140.6, 137.4, 134.3, 129.8, 127, 126.8, 124.3, 123.2, 122.9, 120.1, 119.7, 119.6, 116.1, 1.7.8, 55.2, 40.4, 35.7, 31.7, 31.5, 29.7, 29.1, 23.7, 22.6, 22.6, 14.1, 14. FAB-MS *m/z*: 1003 (M⁺). Anal. Calcd for

SCHEME 1: Synthesis of DTP Oligomers

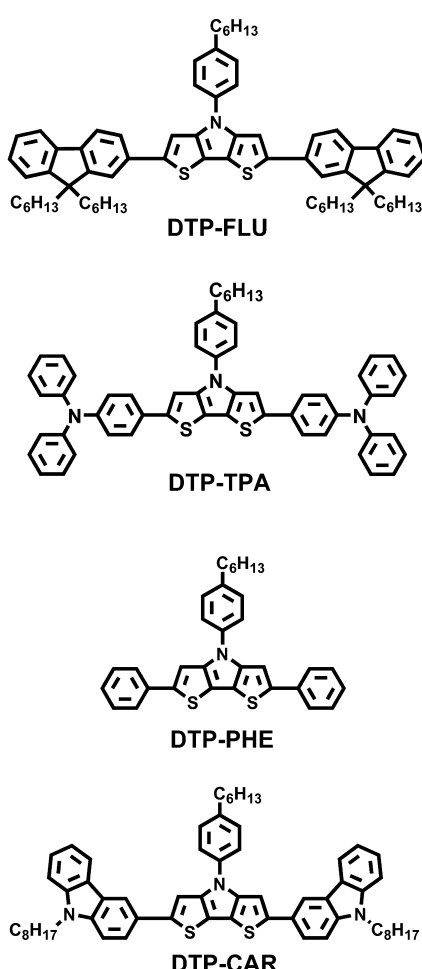


$C_{70}H_{85}NS_2$: C, 83.69; H, 8.53; N, 1.39; S, 6.38. Found: C, 83.74; H, 8.74; N, 1.34; S, 6.33.

2,6-Bis[4-(N,N-diphenylamino)phenyl]-N-(4-hexylphenyl)dithieno[3,2-b;2',3'-d]pyrrole (DTP-TPA). Yellow solid (72%). Melting point: 142–145.2 °C. ¹H NMR (300 MHz, CDCl₃, δ, ppm): 7.52 (d, 8.04 Hz, 3H, Ar–H), 7.35 (b, 9H, Ar–H), 7.25 (b, 4H, Ar–H), 7.14–7.05 (b, 18H, Ar–H), 2.7 (t, 7.56 Hz, 7.89 Hz, 2H, Ar–CH₂), 1.69 (m, 2H, CH₂), 1.35 (m, 6H, CH₂), 0.93 (t, 3H, CH₃). ¹³C NMR (75.4 MHz, CDCl₃, δ, ppm): 147.7, 147.5, 146.7, 141.2, 137.3, 129.7, 129.3, 128.7, 127.7, 127.3, 126.6, 124.9, 124.4, 124.3, 124.1, 123.9, 123, 122.8, 35.5, 31.7, 31.7, 31.5, 29.1, 22.6, 14.1. FAB-MS; *m/z*: 825 (M⁺). Anal. Calcd for C₅₆H₄₇N₃S₂•C₄H₈O₂: C, 78.83; H, 6.06; N, 4.6; O, 3.5; S, 7.01. Found: C, 78.67; H, 6.85; N, 4.2; O, 3.52; S, 7.14.

2,6-Diphenyl-N-(4-hexylphenyl)dithieno[3,2-b;2',3'-d]pyrrole (DTP-PHE). Yellow solid (70%). Melting point: 182.3–184.5 °C. ¹H NMR (300 MHz, CDCl₃, δ, ppm): 7.89 (d, *J* = 7.89 Hz, 4H, Ar–H), 7.54 (d, *J* = 8.37, 2H, Ar–H), 7.39 (m, 8H, Ar–H), 7.29 (m, 1H, Ar–H), 7.24 (m, 1H, Ar–H), 2.71 (t, 2H, *J* = 7.56, Ar–CH₂), 1.7 (m, 2H, –CH₂), 1.34 (m, 6H, –CH₂), 0.92 (t, *J* = 7 Hz, 3H, –CH₃). ¹³C NMR (75.4 MHz, CDCl₃, δ, ppm): 144.2, 142.5, 141.4, 137.2, 135.4, 129.8, 128.9, 127.3, 125.4, 122.9, 116.3, 108.2, 35.6, 31.7, 31.5, 29, 22.6, 14.1. EI-MS *m/z*: 491 (M⁺). Anal. Calcd for C₃₂H₂₉NS₂: C, 78.16; H, 5.94; N, 2.85; S, 13.04. Found: C, 78.34; H, 6.39; N, 2.59; S, 12.74.

2,6-Bis[3,6-(N-2-ethylhexylcarbazole)]-N-(4-hexylphenyl)dithieno[3,2-b;2',3'-d]pyrrole (DTP-CAR). Yellow green solid (63%). Melting point: 69.9–72 °C. ¹H NMR (300 MHz,



CDCl₃, δ, ppm): 8.15 (d, 7.74 Hz, 2H, Ar–H), 7.64 (d, 7.71 Hz, 2H, Ar–H), 7.5–7.4 (m, 9H, Ar–H), 2.74 (t, 7.74 Hz, 7.71 Hz, 2H, Ar–CH₂), 2.1 (b, 2H, N–CH₂), 1.74 (m, 2H, CH₂), 1.44–1.26 (b, 24H, CH₂), 0.96–0.85 (b, 15H, CH₃). FAB-MS *m/z*: 893 (M⁺). Anal. Calcd for C₆₀H₆₇N₃S₂: C, 80.58; H, 7.55; N, 4.7; S, 7.17. Found: C, 80.26; H, 7.75; N, 4.46; S, 7.04.

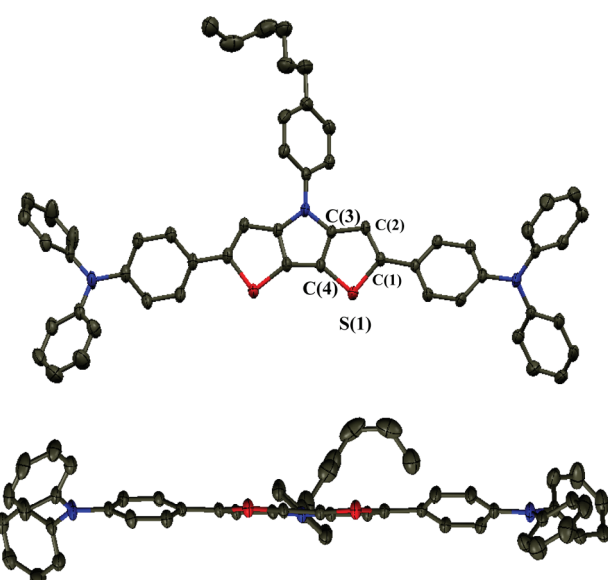


Figure 2. Thermal ellipsoid plot of DTP-TPA with 50% probability.

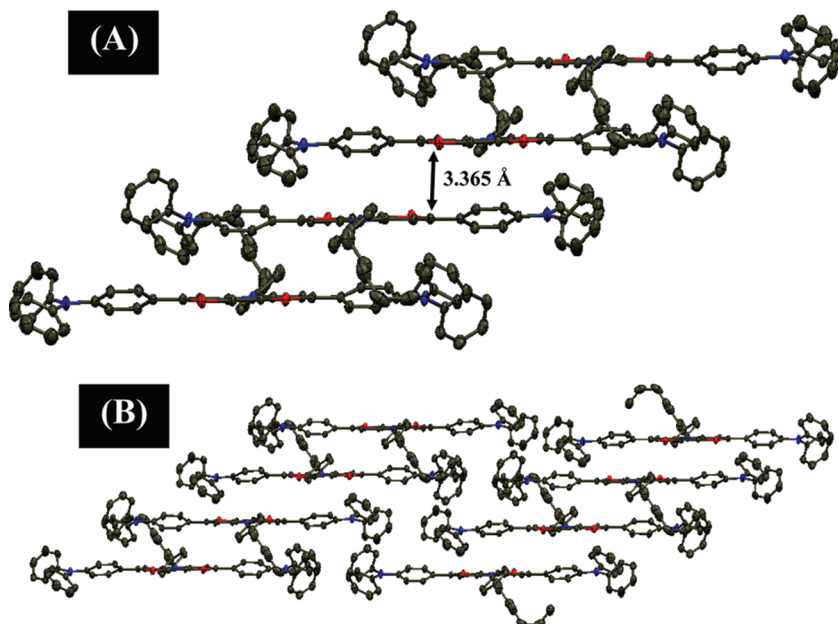


Figure 3. Crystal packing along the *a*-axis (A) and packing of two adjacent columns (B) of DTP-TPA. Hydrogen atoms are removed for clarity.

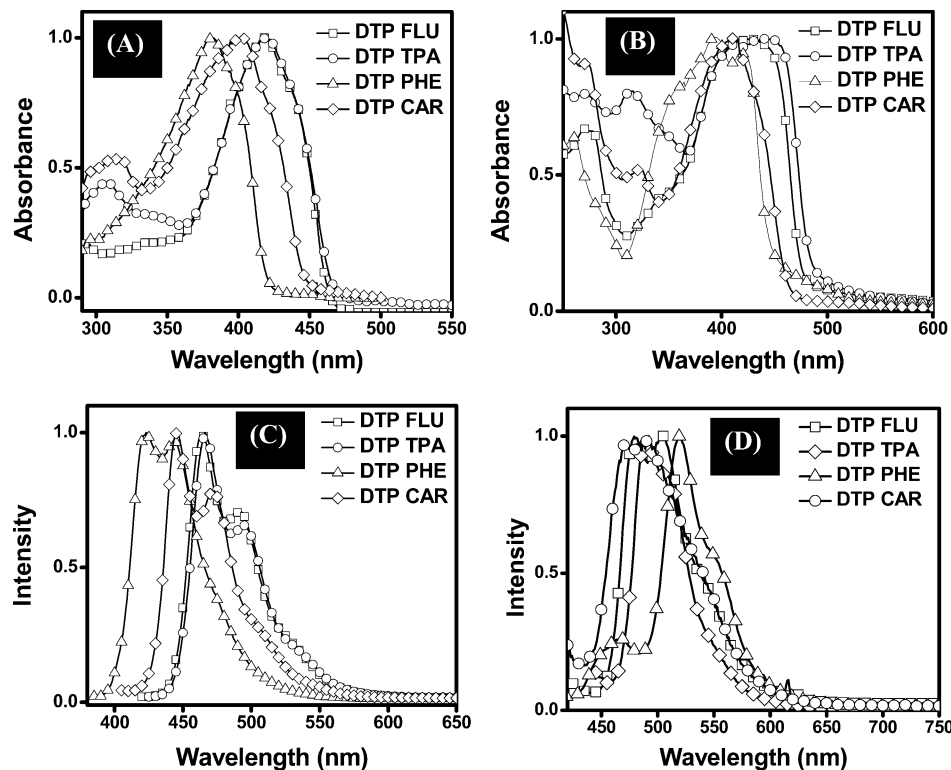


Figure 4. Spectra of absorption in solution (A) and in the solid state (B) and emission in solution (C) and in the solid state (D) of DTP oligomers.

Result and Discussion

Synthesis. Scheme 1 represents the synthetic route towards the target molecules. In the literature, the synthesis of DTP was successfully achieved by two routes. In the first route, DTP was synthesized from 3-bromothiophenes, using a palladium-catalyzed amination reaction followed by copper-catalyzed coupling.^{15a} In order to incorporate different functional groups and the stability of the intermediates, we adopted the second strategy to synthesize the target compounds. In the second route, DTP is conveniently synthesized in good yields from 3,3'-dibromo-2,2'-bithiophene and alkyl/aryl amines via an amination

reaction catalyzed by $\text{Pd}_2(\text{dba})_3$ and $\text{P}(\text{iBu})_3$.¹⁸ Dibromo-DTP was synthesized by brominating DTP with NBS in an acetic acid–chloroform mixture. 9,9-Dihexyl-9H-fluorene-2-boronic acid²¹ and *N*-(2-ethylhexyl)carbazole-2-boronic acid²² were synthesized from 2-bromofluorene and carbazole, respectively, by following the reported procedure. Target oligomers were synthesized in good yields (60–75%) by Suzuki coupling of corresponding boronic acids with dibromo-DTP.

All synthesized oligomers were stable and soluble in common organic solvents such as dichloromethane, chloroform, tetrahydrofuran, and ethylacetate. ^1H NMR spectra, mass spectra,

TABLE 1: Optical Properties of DTP Oligomers in Solution and the Solid State

oligomer	absorption λ_{\max} (nm)		emission λ_{\max} (nm)		QY (%)	
	solution (THF)	thin film	solution (THF)	thin film	solution	thin film
DTP-FLU	416	422	464, 491	481, 505	75%	22%
DTP-TPA	418	438	466, 495	490, 509	70%	10%
DTP-PHE	379	400	423, 444	468, 520	57%	nd ^b
DTP-CAR	401	413	446, 473	485	52%	nd
DTP ^a	310, 300, 293, 261		325		0.28%	

^a Ogawa, K.; Rasmuseen, S. C. *J. Org. Chem.* 2003, 68, 2921. ^b nd: not determined.

elemental analysis, and X-ray single-crystal analysis confirmed the structure of oligomers.

X-ray Crystal Structure. A single crystal of DTP-TPA suitable for single-crystal X-ray diffraction was obtained as a golden yellow crystal via slow evaporation of chloroform solution. A thermal ellipsoid plot of DTP-TPA is shown in Figure 2. This molecule was found to cocrystallize with ethyl acetate (workup solvent) in a triclinic lattice with unit cell parameters of $a = 12.5499(5)$ Å, $b = 14.0994(6)$ Å, $c = 14.8676(6)$ Å, $\alpha = 88.6590(10)$ °, $\beta = 71.1660(10)$ °, and $\gamma = 80.8330(10)$ °. The structures of these molecules are refined to final results of $R1 = 0.0714$ and a goodness of fit of 1.093. The dithienopyrrole unit in DTP-TPA is planar, with the pendant phenyl group twisted to 41°, and the phenyl rings of two triphenylamine units are tilted by 24 and 20° relative to the DTP plane. When compared to the crystal structure of the parent *N*-(4-hexylphenyl)dithieno[3,2-*b*:2',3'-*d*]pyrrole^{15a} S(1)-C(1), S(1)-C(4), and C(1)-C(2) bonds are slightly elongated by 0.041, 0.021, and 0.02 Å, respectively, due to the substitution of triarylamine. The lengthening of these bonds suggests an increase in delocalization of π -electrons within the π -system.

In the solid state, DTP-TPA arranges in slipped π -stacked manner along the *a*-axis with an internuclear distance of 3.37 Å, which equals the sum of van der Waals radii of carbon atoms

(Figure 3). These π -stacked molecules are anticofacially arranged, leading to a one-dimensional structure. The phenyl group of the triphenyl amine unit (attached to DTP) is involved in π -stacking with the DTP core, whereas the other two phenyl groups interact with neighboring columns. Alkyl groups have no effect on the overall packing of the molecule.

Optical Properties. The UV-vis absorption spectra of oligomers in solution as well as those in thin films are shown in Figure 4A, B. All oligomers have strong absorption in the range of 380–420 nm. It is noted that the absorption maxima of all of these oligomers are red-shifted compared to the parent DTP ($\lambda_{\max} = 310$ nm) due to extension of conjugation. Relatively shorter wavelength absorptions of DTP-PHE and DTP-CAR are expected due to shorter conjugation lengths of the attached side group in the former and the nonconjugated position of attachment in the latter. Transparent and uniform films were prepared by spin-coating the chloroform solution of oligomers onto a quartz substrate. Films of all oligomers were yellow-green in color, except DTP-PHE, which was pale green in color. Broad peaks with a bathochromic shift in the absorption were observed for all oligomers in the solid state (Figure 4B). Emission spectra of oligomers were also recorded in solution (THF) and in the film state (Figure 4C, D). In the solution state, all oligomers showed bluish-green emission, with

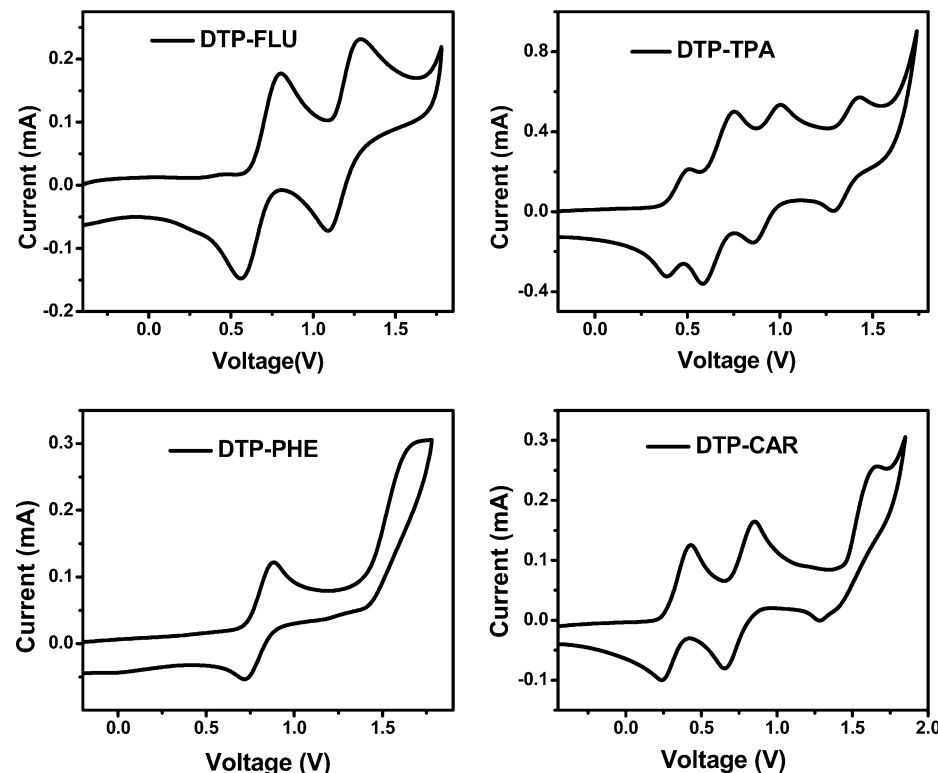


Figure 5. Cyclicvoltammogram of DTP oligomers in dichloromethane containing 0.1 M *n*-Bu₄NPF₆ at the scan rate of 100 mV/s.

TABLE 2: Electrochemical Properties of DTP Oligomers

oligomer	E_{oxid} (V)	$E_{\text{ox onset}}$ (V)	ΔE (V)	E_{HOMO} (eV)	λ_{onset} (nm)	E_g (eV)	E_{LUMO} (eV)
DTP–FLU	0.8, 1.28	0.6	0.24, 0.19	-4.98	483	2.57	-2.41
DTP–TPA	0.49, 0.74, 0.99, 1.42	0.38	0.12, 0.17, 0.16, 0.14	-4.76	486	2.55	-2.21
DTP–PHE	0.88, 1.7	0.73	0.18	-5.11	441	2.81	-2.3
DTP–CAR	0.5, 0.93, 1.73	0.37	0.19, 0.2, 0.38	-4.75	467	2.66	-2.09
DTP ^a	0.65, 1.1						

^a Ogawa, K.; Rasmuseen, S. C. *J. Org. Chem.* 2003, 68, 2921.

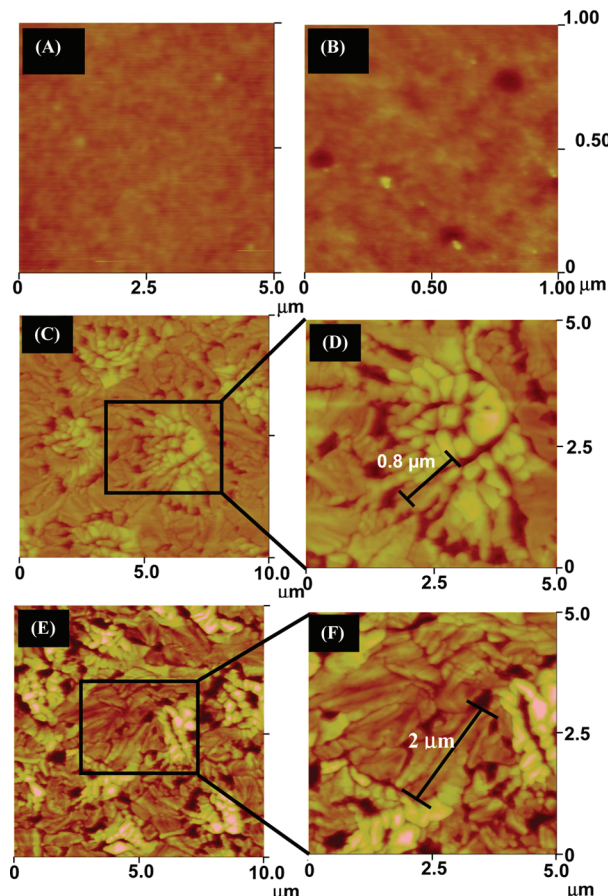


Figure 6. Tapping mode AFM images show the surface morphology of the spin-coated oligomers (A) DTP–CAR ($5 \mu\text{m} \times 5 \mu\text{m}$) and (B) DTP–TPA ($1 \mu\text{m} \times 1 \mu\text{m}$). (C) DTP–PHE ($10 \mu\text{m} \times 10 \mu\text{m}$) and (D) a magnified image of (C) ($5 \mu\text{m} \times 5 \mu\text{m}$). (E) The same sample after annealing at 60°C for 20 min ($10 \mu\text{m} \times 10 \mu\text{m}$) and (F) a magnified image of (E) ($5 \mu\text{m} \times 5 \mu\text{m}$).

emission maxima in the range of 440–490 nm. DTP–PHE showed blue emission at a shorter wavelength than the rest of the oligomers in the series. However, in the solid state, DTP–PHE showed emission at a higher wavelength than the rest of the oligomers. This can be attributed to the close packing of this molecule in the solid state compared to that of other members in the series. Emission spectra of other oligomers in the film state are also red-shifted to give greenish-yellow emission. Interestingly, all synthesized DTP oligomers are highly emissive in nature. The solution state quantum yields of these compounds were calculated in THF with quinine sulfate as the standard. DTP–FLU and DTP–TPA are the two highly fluorescent oligomers in the series with solution-state quantum yields of 75 and 70%, respectively. To the best of our knowledge, this is the highest solution-state quantum yield reported for any DTP system. DTP–PHE and DTP–CAR exhibited comparatively lower quantum yields of 57 and 52%, respectively. Unlike other known thiophene molecules, all

oligomers showed emission in the solid state.²³ The solid-state quantum yields of DTP–FLU and DTP–TPA were measured by using an integrating sphere.²⁴ DTP–FLU exhibited a solid-state quantum yield of 22%, while that of the other emissive analogue DTP–TPA was 10%. From the initial study, it is noted that DTP–FLU and DTP–TPA exhibit very similar photophysical properties. A detailed investigation of the excited-state dynamics of these molecules will provide a better understanding of their photophysical properties. A study in this direction is currently under progress in our laboratory. The low solid-state quantum yield of DTP–TPA compared to that of DTP–FLU may be due to the π -stacking (also indicated by single-crystal X-ray diffraction) which leads to the self-quenching of excited-state species.²⁵ The optical properties of all compounds in solution as well as those in the film state are summarized in Table 1.

Electrochemical Properties. Electrochemical properties of all oligomers were investigated by cyclic voltammetry (Figure 5). Cyclic voltammograms of oligomers were recorded using Pt wire as the working electrode in dichloromethane with 0.1 M *n*-Bu₄NPF₆ as the supporting electrolyte. The CV potentials were measured versus a Ag/AgCl electrode, which was calibrated using a ferrocene/ferrocenium redox couple. No significant changes in the cyclic voltammograms were observed after repeated scanning. More than one quasi-reversible couple was observed for all oligomers with an oxidation peak potential in the range of 0.5–1.75 V versus a Ag/AgCl electrode. DTP–FLU and DTP–PHE showed two oxidation waves at a higher potential (FLU 0.8, 1.28 V, PHE 0.88, 1.7 V) than that of the parent DTP (0.65, 1.1 V).^{15a} For DTP, the second oxidation potential was assigned to the coupling of the thiophene radical cation, which is not the case for substituted DTP oligomers as the substituent blocks the electroactive sites. Oligomers with nitrogen-containing end groups (DTP–CAR and DTP–TPA) exhibited similar electrochemical behavior with multiple oxidation peaks. The first oxidation potentials of DTP–TPA and DTP–CAR were observed at a lower value than those of the parent DTP due to an increase in electron density of the system caused by the triphenylamine and carbazole end groups, respectively.

All electrochemical data, the HOMO energy levels, optical band gaps, and calculated LUMO energy levels are summarized in Table 2. HOMO energy levels were obtained electrochemically from the oxidation onset potential using the empirical formula $E_{\text{HOMO}} = -(E_{\text{ox}} + 4.38)$ eV.²⁶ As we were not able to observe the reduction in these molecules in the scan range, LUMO values were calculated from E_{HOMO} and the optical band gap (E_g). The optical band gap varied from 2.81 (DTP–PHE) to 2.55 eV (DTP–TPA). DTP–FLU and DTP–PHE were found to have a higher oxidation potential and a lower HOMO level with increased stability as compared to those of other members in the series.

Surface Morphology. The morphology of the film sample was characterized by using atomic force microscopy (AFM). The film was prepared by spin-coating the oligomer solution

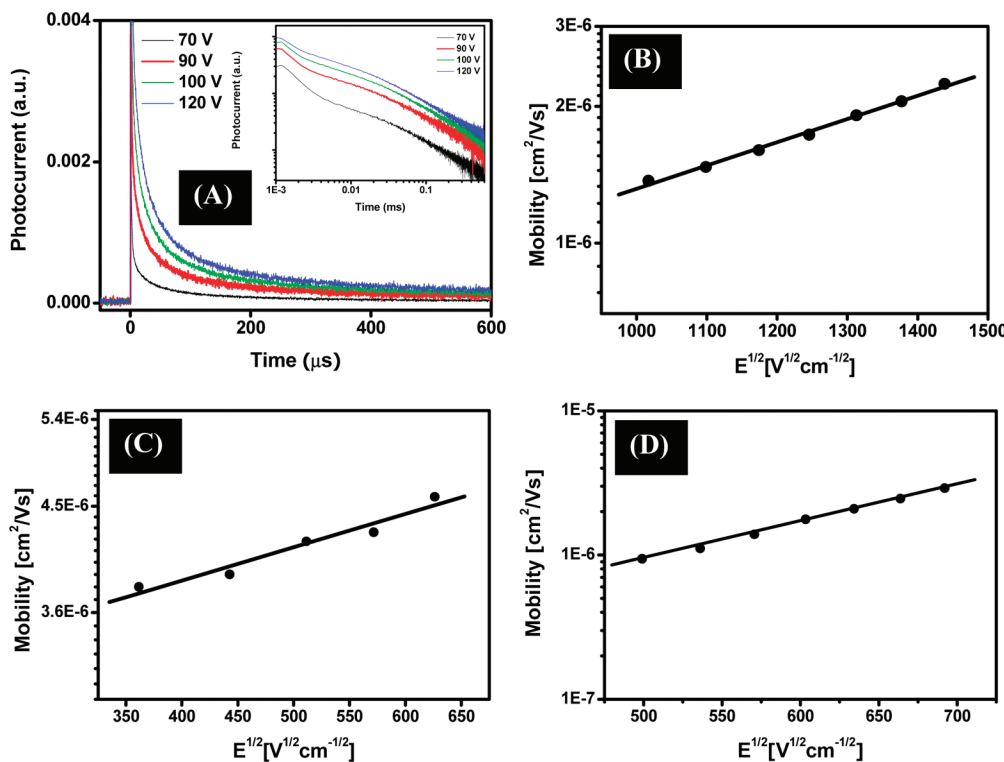


Figure 7. Liner plot (A) of TOF hole transients for DTP–FLU for different applied voltages. Inset: corresponding log–log plot. Variation of TOF hole mobility with applied electric field for DTP–FLU (B), DTP–PHE (C), and DTP–TPA (D); the solid line is a linear fit with Pool–Frenkel equation.

onto an ITO-coated glass substrate. Figure 6 shows the tapping mode AFM images of DTP–CAR, DTP–TPA, and DTP–PHE. DTP–CAR and DTP–TPA form uniform films with rms roughnesses of ~ 1.03 and 2.57 nm, respectively. It can be seen that DTP–PHE forms interconnected crystalline domains with grains of micrometer size. The average grain size was calculated to be around $0.8\ \mu\text{m}$. It was observed that by annealing this sample ($60\ ^\circ\text{C}$ for 20 min), larger crystal domains or crystal grains were formed. In the annealed sample, the average grain size reached up to $\sim 2\ \mu\text{m}$ (see Figure 6E and F).

Charge-Transport Properties. The charge mobility of the oligomers was measured by using a conventional time-of-flight (TOF) photoconductivity technique. The device configuration used for the TOF measurement was ITO/DTP/Al. Film samples of DTP oligomers (thickness: $0.15\ \mu\text{m}$ – $0.6\ \mu\text{m}$) were prepared by drop casting the chloroform solution onto an ITO-coated glass substrate in a solvent-saturated environment. The thickness of the oligomer film was measured by using a surface profiler. A $100\ \text{nm}$ thick aluminum (Al) electrode was evaporated onto the DTP film by using an Edwards thermal evaporator. The charge mobilities were calculated using the relation $\mu = d^2/Vt_T$, where d is the thickness of the film, V is the applied voltage, and t_T is the transit time.

Figure 7A shows the linear plot of TOF hole transients obtained for DTP–FLU, and the inset represents the corresponding double logarithmic plot. The material was found to be hole-transporting in nature. In this case, the transit time was obtained from the inflection point in the double logarithmic plot of the photocurrent versus time. The variation of hole mobility with the applied electric field for DTP–FLU is shown in Figure 7B. The hole mobility was found to be $2.1 \times 10^{-6}\ \text{cm}^2/(\text{V s})$ at an applied electric field of $1.9 \times 10^6\ \text{V/cm}$. The zero field mobility, which is a valuable parameter in many applications, was extracted from the Pool–Frenkel fit ($\mu = \mu_{(E=0)} \exp(\gamma E^{1/2})$), and it was found to be $4 \times 10^{-7}\ \text{cm}^2/(\text{V s})$. Figure 7C, D represents the

TABLE 3: Hole Mobility of DTP Oligomers

oligomer	mobility ($\text{cm}^2/(\text{V s})$)	zero field mobility ($\text{cm}^2/(\text{V s})$)	γ ($\text{cm}/\text{V})^{1/2}$
DTP–FLU	2.1×10^{-6} (field: $1.9 \times 10^6\ \text{V/cm}$)	4×10^{-7}	5.1×10^{-4}
DTP–TPA	2.09×10^{-6} (field: $4.0 \times 10^5\ \text{V/cm}$)	4.6×10^{-8}	2.6×10^{-3}
DTP–PHE	4.2×10^{-6} (field: $2.6 \times 10^5\ \text{V/cm}$)	2.9×10^{-6}	3.04×10^{-4}
DTP–CAR	nd ^a	nd	nd

^a nd: not determined.

variation of hole mobility with applied electric field in DTP–PHE and DTP–TPA, respectively. In the case of DTP–PHE, the transit time was extracted by the integration method,²⁷ and in DTP–TPA, it was obtained from the log–log plot. For DTP–PHE and DTP–TPA, the hole mobilities were found to be 4.2×10^{-6} (field = $2.6 \times 10^5\ \text{V/cm}$) and $2.09 \times 10^{-6}\ \text{cm}^2/(\text{V s})$ (field = $4 \times 10^5\ \text{V/cm}$), respectively. The zero field mobility was calculated from the Pool–Frenkel plot, and it was found to be 2.9×10^{-6} and $4.6 \times 10^{-8}\ \text{cm}^2/(\text{V s})$ for DTP–PHE and DTP–TPA, respectively. In the case of DTP–CAR, the photocurrent was very weak; therefore, it was difficult to obtain accurate hole mobility. The charge-transport parameters of all of the oligomers are summarized in Table 3. It is noteworthy that the hole mobilities of all DTP oligomers are in good agreement with the Pool–Frenkel relationship.²⁸ Also, the hole mobility values of these DTP oligomers are similar to that of MEH–PPV (hole mobility $\approx 10^{-6}\ \text{cm}^2/(\text{V s})$), which was successfully tested for OLED applications.²⁹

Conclusion

A new series of DTP-incorporated oligomeric systems with phenyl, fluorene, triphenylamine, and carbazole units was

synthesized and characterized. The crystal structure and crystal packing of DTP–TPA were studied. DTP–TPA packed in the π -stacked manner with a distance of 3.37 Å. The oligomer DTP–PHE showed a blue emission with the solution-state quantum yield of 57%. All other oligomers showed green emission with a quantum yield of 52–75%. DTP–FLU exhibited a high solution quantum yield of 75% and a solid-state quantum yield of 22%. A higher oxidation potential and the low-lying HOMO of DTP–FLU and DTP–PHE compared to those of the other two members in the series indicate a higher stability of these compounds. The materials are found to be hole-transporting, and the mobilities of the charge carriers were measured by using the time-of-flight technique. The hole mobilities were found to be on the order of 10^{-6} cm²/(V s). The high fluorescence nature of DTP–FLU and DTP–TPA in the solid state and the reversible electrochemical property indicate the potential for these oligomers in optoelectronic applications.

Acknowledgment. The authors would like to thank the Agency for Science, Technology and Research (A*STAR) and the National University of Singapore for financial support. The authors would also like to thank Miss Tan Geok Kheng for the X-ray crystal diffraction experiment and data refinement and Ms. Sajini Vadukumpally and Mr. Surani b Dolmanan for the technical assistance with the AFM and solid-state quantum yield measurements.

Supporting Information Available: ¹H NMR, mass spectrum of oligomers, crystal data in CIF format, and TOF photocurrent transients. This material is available free of charge via the Internet at <http://pubs.acs.org>.

References and Notes

- (1) (a) Sirringhaus, H.; Tessler, N.; Friend, R. H. *Science* **1998**, 280, 1741. (b) Garnier, F.; Hajlaoui, R.; Yassar, A.; Srivastava, P. *Science* **1994**, 265, 1684.
- (2) (a) *Handbook of Oligo- and Polythiophene*; Fichou, D., Ed.; Wiley-VCH: Weinheim, Germany, 1999. (b) *Electronic Materials: The Oligomer Approach*; Müllen, K., Wegner, G., Eds.; Wiley-VCH: Weinheim, Germany, 1998.
- (3) Roncali, J. In *Handbook of Conducting Polymers*, 2nd ed.; Skotheim, T. A., Elsenbaumer, R. L., Reynolds, J. R., Eds.; Marcel Dekker: New York, 1998; Chapter 12.
- (4) (a) Ohmori, Y.; Uchida, M.; Muro, K.; Yoshino, K. *Solid State Commun.* **1991**, 80, 605. (b) Braun, D.; Gustaffson, G.; McBranch, D.; Heeger, A. J. *J. Appl. Phys.* **1992**, 72, 564. (c) Andersson, M. R.; Thomas, O.; Mammo, W.; Svensson, M.; theander, M.; Inganäs, O. *J. Mater. Chem.* **1999**, 9, 1933. (d) Gigli, G.; Barbarella, G.; Favaretto, L.; Cacialli, F.; Cingolani, R. *Appl. Phys. Lett.* **1999**, 75, 439. (e) Perepichka, I. F.; Perepichka, D. F.; Meng, H.; Wudl, F. *Adv. Mater.* **2005**, 17, 2281.
- (5) (a) Murphy, A. R.; Fréchet, J. M. J.; Chang, P.; Lee, J.; Subramanian, V. *J. Am. Chem. Soc.* **2004**, 126, 1596. (b) Chang, P. C.; Lee, J.; Huang, D.; Subramanian, V.; Murphy, A. R.; Fréchet, M. *J. Chem. Mater.* **2004**, 16, 4783. (c) Letizia, J. A.; Faccetti, A.; Stern, C. L.; Ratner, A.; Marks, T. *J. Am. Chem. Soc.* **2005**, 127, 13476.
- (6) (a) Campos, L. M.; Tontchev, A.; Güness, S.; Sonmez, G.; Neugebauer, H.; Sariciftci, N. S.; Wudl, F. *Chem. Mater.* **2005**, 17, 4031. (b) Sonmez, G. *Chem. Commun.* **2005**, 5251. (c) Wienk, M. M.; Turbiez, M. G. R.; Struijk, M. P.; Fonrodona, M.; Janseen, R. A. J. *Appl. Phys. Lett.* **2006**, 88, 153511(1).
- (7) (a) Stoyanovioh, F. M.; Federov, B. P. Z. *Org. Khim.* **1965**, 1, 1282. (b) Janssen, M. J.; De Jong, F. *J. Org. Chem.* **1971**, 36, 1645. (c) Taliani, C.; Danieli, R.; Zamboni, R.; Ostoja, P.; Porzio, W. *Synth. Met.* **1987**, 18, 177. (d) Jow, T. R.; Jen, K. Y.; Elsenbaumer, R. L.; Shacklette, L. W.; Angelopoulos, M.; Cava, M. P. *Synth. Met.* **1986**, 14, 53. (e) Di Marco, P.; Mastragostino, M.; Taliani, C. *Mol. Cryst. Liq. Cryst.* **1985**, 118, 241.
- (8) (a) Coppo, P.; Tuner, M. L. *J. Mater. Chem.* **2005**, 15, 1123. (b) Zotti, G.; Schiavon, G.; Berlin, A.; Fontana, G.; Pagani, G. *Macromolecules* **1994**, 27, 1938. (c) Benincori, T.; Consonni, V.; Gramatica, P.; Pilati, T.; Rizzo, S.; Sannicolo, F.; Todeschini, R.; Zotti, G. *Chem. Mater.* **2001**, 13, 1665. (d) Zotti, G.; Zecchin, S.; Schiavon, G.; Berlin, A. *Macromolecules* **2001**, 34, 3889. (e) Sannicolo, F.; Brenna, E.; Benincori, T.; Zotti, G.; Zecchin, S.; Schiavon, G.; Pilati, T. *Chem. Mater.* **1998**, 10, 2167. (f) Coppo, P.; Cupertino, D. C.; Yeates, S. G.; Turner, M. L. *Macromolecules* **2003**, 36, 2705. (g) Asawapirom, U.; Scherf, U. *Macromol. Rapid Commun.* **2001**, 22, 746.
- (9) (a) Zanirato, P.; Spagnolo, P.; Zanardi, G. *J. Chem. Soc., Perkin Trans. 1* **1983**, 2551. (b) Berlin, A.; Pagani, G.; Zotti, G.; Chiavon, G. *Makrolol. Chem.* **1992**, 193, 399. (c) Beggiato, G.; Casalbore-Miceli, G.; Geri, A.; Berlin, A.; Pagani, G. *Synth. Met.* **1996**, 82, 11. (d) Berlin, A.; Zotti, G.; Schiavon, G.; Zecchin, S. *J. Am. Chem. Soc.* **1998**, 120, 13453. (e) Laks, B.; Del Nero, J. *Synth. Met.* **1999**, 101, 379. (f) Zotti, G.; Berlin, A.; Schiavon, G.; Zecchin, S. *Synth. Met.* **1999**, 101, 622. (g) Nero, J. D.; Laks, B. *J. Mol. Model.* **2001**, 354.
- (10) Baumgartner, T. *J. Inorg. Organomet. Polym.* **2006**, 15, 389.
- (11) (a) Li, X.-C.; Sirringhaus, H.; Garnier, F.; Holmes, A. B.; Moratti, S. C.; Feeder, N.; Clegg, W.; Teat, S. J.; Friend, R. H. *J. Am. Chem. Soc.* **1998**, 120, 2206. (b) Coppo, P.; Tuner, M. L.; Cupertino, D. C.; Yeates, S. G. *Mater. Res. Soc. Symp. Proc.* **2003**, 771, 61. (c) Sun, Y. M.; Ma, Y. Q.; Liu, Y. Q.; Lin, Y. Y.; Wang, Z. Y.; Wang, Y.; Di, C. A.; Xiao, K.; Chen, X. M.; Qiu, W. F.; Zhang, B.; Yu, G.; Hu, W. P.; Zhu, D. B. *Adv. Funct. Mater.* **2006**, 16, 426. (d) Moulé, A. J.; Tsami, A.; Bünnagel, T.; Forster, M.; Kronenberg, N. M.; Scharber, M.; Koppe, M.; Morana, M.; Brabec, C. J.; Meerholz, K.; Scherf, U. *Chem. Mater.* **2008**, 20, 4045.
- (12) Berlin, A.; Pagani, G. A.; Sannicolo, F.; Schiavon, G.; Zotti, G. *Polymer* **1991**, 32, 1841.
- (13) (a) Belcher, W. J.; Rasmussen, S. C.; Dastoor, P. C. *Polym. Prepr.* **2007**, 48, 11. (b) Zhou, E.; Nakamura, M.; Nishizawa, T.; Zhang, Y.; Wei, Q.; Tajima, K.; Yang, C.; Hashimoto, K. *Macromolecules* **2008**, 41, 8302. (c) Steckler, T. T.; Zhang, X.; Hwang, J.; Honeyager, R.; Ohira, S.; Zhang, X.-H.; Grant, A.; Ellinger, S.; Odom, S. A.; Sweat, D.; Tanner, D. B.; Rinzler, A. G.; Barlow, S.; Brédas, J. L.; Kippelen, B.; Marder, S. R.; Reynolds, J. R. *J. Am. Chem. Soc.* **2009**, 131, 2824.
- (14) (a) Liu, J.; Zhang, R.; Sauvé, G.; Kowalewki, T.; McCullough, R. D. *J. Am. Chem. Soc.* **2008**, 130, 13167. (b) Zhang, W.; Li, J.; Zhang, B.; Qin, J.; Lu, Z.; P. Y.; Mary, B.; Chan-Park; Li, C. M. *Macromolecules* **2008**, 41, 8953.
- (15) (a) Ogawa, K.; Rasmussen, S. C. *J. Org. Chem.* **2003**, 68, 2921. (b) Fujitsuka, M.; Sato, T.; Sezaki, F.; Tanaka, K.; Watanabe, A.; Ito, O. *J. Chem. Soc., Faraday Trans.* **1998**, 94, 3331.
- (16) (a) Radke, K. R.; Ogawa, K.; Rasmussen, S. C. *Org. Lett.* **2005**, 7, 5253. (b) Mo, H.; Rasmussen, S. C. *Polym. Prepr.* **2007**, 48, 61. (c) Ogawa, K.; Mo, H.; Radke, K. R.; Rasmussen, S. C. *Polym. Prepr.* **2007**, 48, 40. (d) Ogawa, K.; Rasmussen, S. C. *Macromolecules* **2006**, 39, 1771.
- (17) Zhang, W.; Li, J.; Zhang, B.; Qin, J. *Macromol. Rapid Commun.* **2008**, 29, 1603.
- (18) Odom, S. A.; Lancaster, K.; Beverina, L.; Lefler, K. M.; Thompson, N. J.; Coropceanu, V.; Brédas, J.-L.; Marder, S. R.; Barlow, S. *Chem.—Eur. J.* **2007**, 13, 9637.
- (19) Crosby, G. A.; Demas, J. N. *J. Phys. Chem.* **1971**, 75, 991.
- (20) Vijila, C.; Balakrishnan, B.; Huang, C.; Chen, Z.-K.; Zhen, C.-G.; Auch, M. D. J.; Chua, S. J. *Chem. Phys. Lett.* **2005**, 414, 393.
- (21) Perepichka, I. I.; Perepichka, I. F.; Bryce, M. R.; Palsson, L.-O. *Chem. Commun.* **2005**, 3397.
- (22) (a) Feng, G. L.; Lai, W. Y.; Ji, S. J.; Huang, W. *Tetrahedron Lett.* **2006**, 47, 7089. (b) Zhang, K.; Chen, Z.; Yang, C.; Zhang, X.; Tao, Y.; Duan, L.; Chen, L.; Zhu, L.; Qin, J.; Cao, Y. *J. Mater. Chem.* **2007**, 17, 3451.
- (23) Beljonne, D.; Cornil, J.; Friend, R. H.; Janssen, R. A. J.; Bredas, J. L. *J. Am. Chem. Soc.* **1996**, 118, 6453.
- (24) de Mello, J. C.; Wittmann, H. F.; Friend, R. H. *Adv. Mater.* **1997**, 9, 230.
- (25) (a) Rothberg, L. J.; Yan, M.; Papadimitrakopoulos, F.; Galvin, M. E.; Kwock, E. W.; Miller, T. M. *Synth. Met.* **1996**, 80, 41. (b) Peng, Z. *Polym. News* **2000**, 25, 185. (c) Ashraf, R. S.; Shahid, M.; Klemm, E.; Al-Ibrahim, M.; Senfuss, S. *Macromol. Rapid Commun.* **2006**, 27, 1454.
- (26) (a) Leeuw, D. M.; Simenon, M. M. J.; Brown, A. R.; Einerhand, R. E. F. *Synth. Met.* **1997**, 87, 53. (b) Cui, Y.; Zhang, X.; Jenke, S. A. *Macromolecules* **1999**, 32, 3824. (c) Li, Y.; Ding, J.; Day, M.; Tao, Y.; Lu, J.; D'iorio, M. *Chem. Mater.* **2004**, 16, 2165.
- (27) Campbell, A. J.; Bradley, D. D. C. *Appl. Phys. Lett.* **2001**, 79, 2133.
- (28) Borsenberger, P. M.; Pautmeier, L.; Bässler, H. *J. Chem. Phys.* **1991**, 94, 5447.
- (29) Igno, A. R.; Tan, C. H.; Fann, W.; Huang, Y. S.; Perng, G. Y.; Chen, S. *Adv. Mater.* **2001**, 13, 504.